

Maximum reproductive rate of fish at low population sizes

Ransom A. Myers, Keith G. Bowen, and Nicholas J. Barrowman

Abstract: We examine a database of over 700 spawner-recruitment series to search for parameters that are constant, or nearly so, at the level of a species or above. We find that the number of spawners produced per spawner each year at low populations, i.e., the maximum annual reproductive rate, is relatively constant within species and that there is relatively little variation among species. This quantity can be interpreted as a standardized slope at the origin of a spawner-recruitment function. We employ variance components models that assume that the log of the standardized slope at the origin is a normal random variable. This approach allows improved estimates of spawner-recruitment parameters, estimation of empirical prior distributions for Bayesian analysis, estimation of the biological limits of fishing, calculation of the maximum sustainable yield, and impact assessment of dams and pollution.

Résumé : Nous étudions une base de données comptant plus de 700 séries géniteur-recrutement à la recherche de paramètres qui sont constants, ou presque, au niveau de l'espèce ou à un niveau hiérarchique supérieur. Nous avons trouvé que le nombre de géniteurs produits par géniteur chaque année dans des populations peu abondantes, c'est-à-dire le taux de reproduction annuel maximal, est relativement constant dans une espèce, et qu'il y a peu de variation d'une espèce à l'autre. Cette valeur peut être interprétée comme une pente normalisée à l'origine d'une fonction géniteur-recrutement. Nous avons recours à des modèles de composantes de la variance selon lesquels le log de la pente normalisée à l'origine est une variable aléatoire normale. Cette approche permet d'obtenir de meilleures estimations des paramètres du rapport géniteur-recrutement, une estimation des données empiriques avant les répartitions pour l'analyse bayésienne, une estimation des limites biologiques de la pêche, un calcul de la production maximale équilibrée, et une évaluation des impacts des barrages et de la pollution.

[Traduit par la Rédaction]

Introduction

Perhaps the most fundamental parameter in population biology is the reproductive rate at low population size. We will analyze this parameter in terms of the maximum reproductive rate, which we define as the average rate at which replacement spawners are produced per spawner at low abundance in the absence of anthropogenic mortality (after a time delay for the age at maturity). The maximum reproductive rate is central to the following: the population growth rate r (Cole 1954; Pimm 1991; Myers et al. 1997b), limits to overfishing (Mace 1994; Cook et al. 1997; Myers and Mertz 1998), estimation of the dynamic behaviour of the population, i.e., whether the population has oscillatory or chaotic behaviour, extinction models and population viability analysis (Lande et al. 1997), establishment of biological reference points for management, e.g., most of the commonly used reference points for recruitment overfishing require estimates of the maximum lifetime reproductive rate (Myers et

al. 1994), and estimation of the long-term consequence of mortality caused by pollution, dams, or entrainment by powerplants (Barnthouse et al. 1988).

The purposes of this paper are (*i*) to provide a comprehensive analysis of the maximum reproductive rate in terms of a relatively simple statistical model, (*ii*) to attempt to determine under what conditions this parameter is invariant, i.e., constant for a species or group of species, and (*iii*) to provide empirical Bayesian priors for the estimates (Hilborn and Liermann 1998; Millar and Meyer 2000). We use the extensive database of stock and recruitment data compiled in Myers et al. (1995) and Myers and Barrowman (1996).

Formulation

Estimating reproductive rate

Semelparous species, whose members conveniently die after reproduction, immensely simplify the lives of students of their population biology. For example, in many insects and in pink salmon (*Oncorhynchus gorbuscha*), one generation follows the next in easy units, e.g., the number of spawning females. The relationship between the numbers in year t , N_t , and the numbers in year t plus the age at maturity, a_{mat} , is typically given in the form

$$(1) \quad N_{t+a_{\text{mat}}} = \alpha N_t e^{-f(N_t)}$$

where the density-dependent mortality, $f(N_t)$, is a non-negative function such that $f(N_t) \rightarrow 0$ as $N_t \rightarrow 0$.

Received June 1, 1999. Accepted September 24, 1999.
J15156

R.A. Myers.¹ Killam Memorial Chair in Ocean Studies, Department of Biology, Dalhousie University, Halifax, NS B3H 4J1, Canada.

K.G. Bowen and N.J. Barrowman. Department of Mathematics and Statistics, Dalhousie University, Halifax, NS B3H 4J1, Canada.

¹Author to whom all correspondence should be addressed.
email: ransom.myers@dal.ca

The dynamics of iteroparous species are more complicated. Typically, the number of recruits belonging to year-class t , R_t , is a function of the egg production or a proxy such as weight of spawners at time t , S_t , as in the form

$$(2) \quad R_t = \alpha S_t e^{-f(S_t)}$$

where $f(S_t)$ is the density-dependent mortality as before.

The Ricker model has the form

$$(3) \quad R_t = \alpha S_t e^{-\beta S_t}$$

where α is the slope at the origin (measured perhaps in recruits per kilogram of spawners). Density-dependent mortality is assumed to be the product of β and the spawner biomass. Dividing by S_t and taking logarithms gives

$$(4) \quad \log \frac{R_t}{S_t} = \log \alpha - \beta S_t$$

i.e., a linear model for log survival.

For the forthcoming calculations, the slope at the origin, α , must be standardized. First consider

$$\hat{\alpha} = \alpha \cdot \text{SPR}_{F=0}$$

where $\text{SPR}_{F=0}$ is the spawning biomass resulting from each recruit (perhaps in units of kilograms of spawners per recruit) in the limit of no fishing mortality ($F = 0$). This quantity, $\hat{\alpha}$, represents the number of spawners produced by each spawner over its lifetime at very low spawner abundance, i.e., assuming absolutely no density dependence. The quantity $\tilde{\alpha}$ required for our calculations is the number of spawners produced by each spawner per year (after a lag of a years, where a is the age at maturity). If adult survival (the proportion surviving each year, which in the absence of fishing is e^{-M}) is p_s , then $\tilde{\alpha} = \sum_{i=0}^{\infty} p_s^i \hat{\alpha}$, or summing the geometric series:

$$(5) \quad \tilde{\alpha} = \hat{\alpha}(1 - p_s) = \alpha \cdot \text{SPR}_{F=0}(1 - p_s).$$

This quantity $\tilde{\alpha}$ is the maximum annual reproductive rate and will be the main focus of this study.

A word of warning is needed in the interpretation of the maximum annual reproductive rate. The above formulation is for the deterministic case. However, if stochastic variations in survival are included, then the quantity $\tilde{\alpha}$ would be interpreted as the maximum of the average annual reproductive rate. In other words, the reproductive rate may be higher or lower for any given year.

We also provide estimates of "steepness", denoted by z and first defined by Mace and Doonan (1988), because this is the parameter actually used in many assessments (Hilborn and Walters 1992). The steepness parameter z for the Beverton–Holt model is defined to be the proportion of recruitment, relative to the recruitment at the equilibrium with no fishing, when the spawner abundance or biomass is reduced to 20% of the virgin level. This is related to the maximum lifetime reproductive rate $\hat{\alpha}$ by

$$z = \frac{\hat{\alpha}}{4 + \hat{\alpha}}$$

where $0.2 < z < 1$.

Note that at the limit of small population size, the Ricker and Beverton–Holt models coincide, i.e., the slope at the origin, α , is the same. In this context, z can be estimated from either model; however, it can only be applied directly to the dynamics of the Beverton–Holt model. Our estimate of steepness should be viewed as conservative (see Appendix 2).

To summarize, we have introduced notations for the three most common ways that the maximum reproductive rate is used in the analysis of fish population dynamics. First, we have defined $\hat{\alpha}$ to be the maximum lifetime reproductive rate (the adjective "lifetime" would not usually be used but is important here). This quantity is used in many calculations to determine maximum sustainable yield (MSY) and the limits of fishing mortality. The second is the quantity of steepness, z , which is a simple transformation of $\hat{\alpha}$. The third quantity, $\tilde{\alpha}$, is used in calculations where an annual recruitment rate is needed, e.g., for estimating the maximum population growth rate (Myers et al. 1997b).

The Ricker model provides a reasonable model for estimating the slope at the origin

The simplest form of density-dependent mortality is linear, i.e., $f(S) = \beta S$, in eq. 1. We will show that under reasonable conditions, this is perhaps the best first approximation. A simple generalization of the Ricker model is

$$(6) \quad f(S) = \beta S^\gamma$$

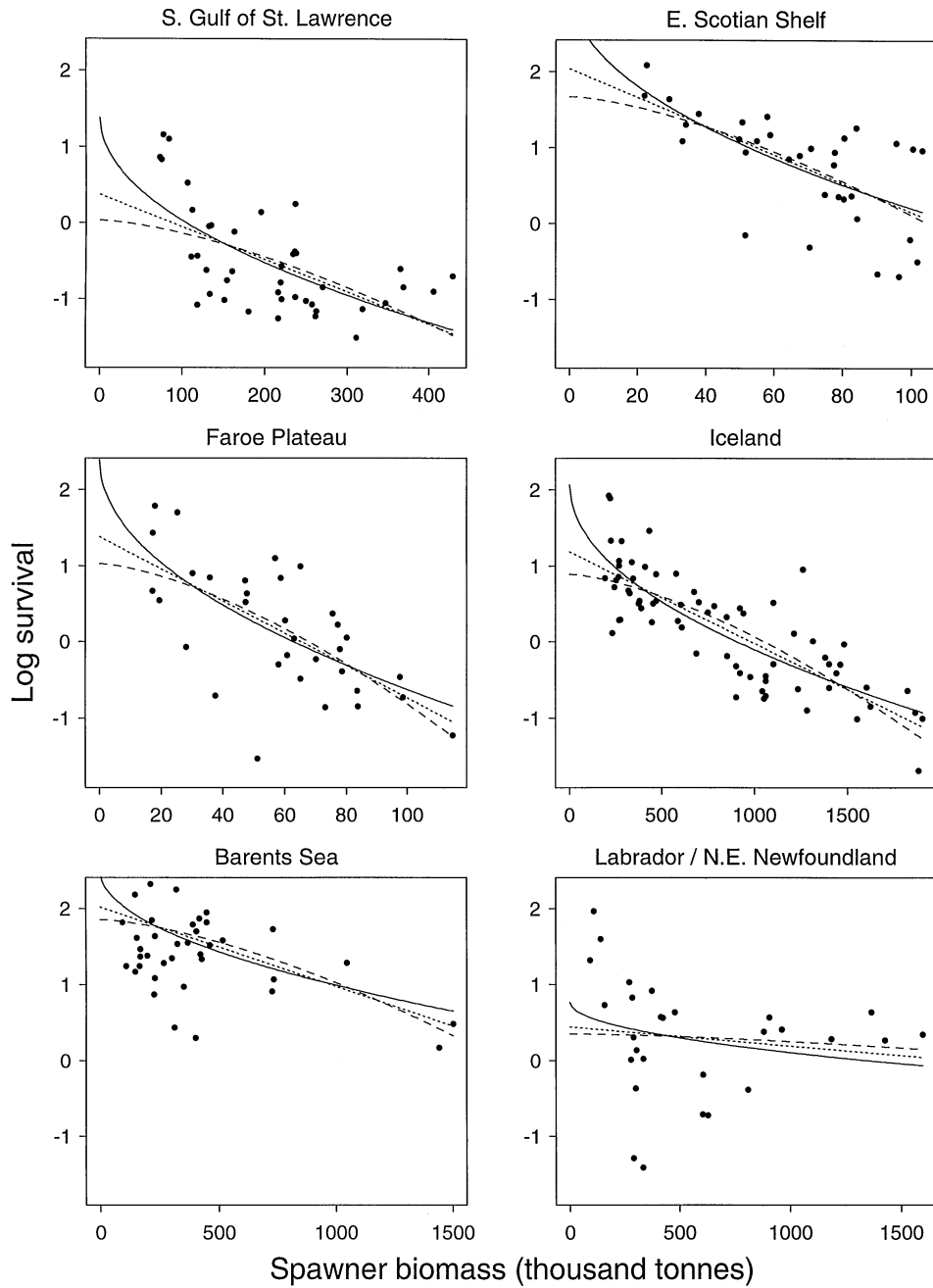
where γ controls the degree of nonlinearity in the functional form of density dependence (Bellows 1981). For most of the data sets that we examine, there are not sufficient data to estimate γ ; however, our purpose is only to ensure that estimates of α are robust to our assumptions about γ . We will examine data for Atlantic cod (*Gadus morhua*) because there are excellent data for these populations and all have been reduced to low levels, which will enhance our ability to estimate α . We held γ fixed at values of 0.5, 0.75, 1, 1.25, and 1.5 (Figs. 1 and 2) and estimated $\tilde{\alpha}$ and β .

The functional fits are displayed in terms of survival ($\log(R/S)$) versus S , where R has been multiplied by $\text{SPR}_{F=0}(1 - p_s)$.

If $\gamma < 1$, then survival is a convex function of spawner biomass, and the limit of survival is infinity as $S \rightarrow 0$. Thus, this model is unrealistic for this case. Furthermore, an examination of the survival versus spawner curve reveals that it does not become appreciably convex until below the lowest observed spawner abundance (Fig. 1). For $\gamma > 1$, survival is a concave function, and the derivative of survival as $S \rightarrow 0$ will always be zero.

In practice, the Ricker model is a reasonably cautious estimate of the limit for management purposes. If $\gamma < 1$ is assumed, then a greater α is estimated, while the assumption of $\gamma > 1$ results in only a slight decrease in the estimate of α (Figs. 1 and 2). If we examine the four cod populations with the largest range in observed spawner biomass, the estimate of the slope at the origin appears reasonable in all cases for the Ricker model, while the estimate for $\gamma = 0.5$ is inflated commensurately with the gap between the origin and the lowest observation of spawner abundance.

Fig. 1. Survival, $\log(R/S)$, versus spawner abundance for six cod stocks. The modeled density-dependent mortality of the form $f(S) = \beta S^\gamma$ is shown for $\gamma = 1.5$ (dashed line), $\gamma = 1$ (Ricker case, dotted line), and $\gamma = 0.5$ (solid line). We have standardized recruitment by multiplying by $\text{SPR}_{F=0}(1 - p_s)$, which allows survival to be interpreted as the annual replacement of spawners per spawner. Thus, the extrapolation of the fitted curves to zero spawner abundance provides an estimate of $\log \tilde{\alpha}$, i.e., the logarithm of the maximum annual reproductive rate.



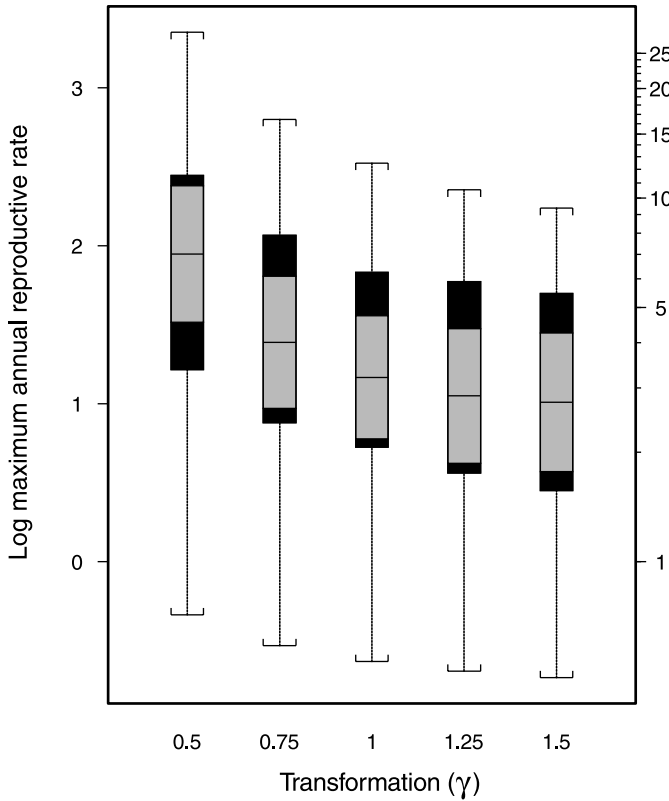
We also considered another common three-parameter model, the "Shepherd function," i.e.:

$$(7) \quad R = \frac{\alpha S}{1 + (S/K)^\delta}.$$

This model was first proposed by Maynard Smith and Slatkin (1973) and was discussed by Bellows (1981). The parameter K has dimensions of biomass and may be interpreted as the "threshold biomass" for the model. For values

of biomass S greater than the threshold K , density-dependent effects dominate. The parameter δ may be called the "degree of compensation" of the model, since it controls the degree to which the (density-independent) numerator is compensated for by the (density-dependent) denominator. If $\delta = 1$, then the Beverton-Holt model is recovered. However, for $\delta < 1$, survival is infinity as $S \rightarrow 0$; again, in this case the model cannot be considered as a reliable method for extrapolation to low population sizes. For $\delta > 1$, the derivative of survival as $S \rightarrow 0$ will always be zero. However, even in the

Fig. 2. Box plots of the logarithm of the scaled slope at the origin, $\log \tilde{\alpha}$, for the 20 major cod stocks in the North Atlantic as a function of the form of density-dependent mortality $f(S) = \beta S^\gamma$. For each box plot, the median is marked with a white line and the gray area shows the 95% confidence interval for the median location. When $\gamma = 1$, the Ricker model is recovered.



Beverton–Holt case ($\delta = 1$), many estimates of the slope at the origin will be infinity. That is, if $K \rightarrow 0$, then $\alpha \rightarrow \infty$ is a perfectly feasible solution.

The Deriso–Schnute model (Hilborn and Walters 1992), an alternative three-parameter model, has the Ricker and the Beverton–Holt as special cases. However, it suffers from the same problems that we described above: survival is not constrained to be finite except when the model is a Ricker model, or it has the derivative of survival as $S \rightarrow 0$ constrained to be zero.

Any estimation of the slope at the origin is necessarily an extrapolation, since there cannot be observations arbitrarily close to zero spawner abundance. The simplest extrapolation is a linear one (in the relationship between log survival and spawner abundance), while alternative assumptions will often produce unreasonable estimates.

One situation in which a Ricker model would not give a reliable estimate would be if mortality increased at low spawner abundances, known as depensation or the Allee effect. Myers et al. (1995) carried out a metaanalysis and could find no convincing evidence that depensation occurred for exploited fish populations. However, Liermann and Hilborn (1997), using a Bayesian approach, demonstrated that the data were consistent with moderate levels of depensation for several taxa. We conclude that the estimate of the α from the Ricker model will usually provide a reasonable estimate for both ecological and management needs, e.g., when F_τ (sometimes called $F_{\text{extinction}}$), the smallest fishing mortality associated with extinction, is needed.

In this section, we have argued that the Ricker model is often a reasonable model for the estimation of the $\tilde{\alpha}$ (some alternative approaches are discussed below). For the cod populations in the North Atlantic, we have seen that the estimates are only slightly modified if survival is a concave function of spawner biomass. The alternative assumption, that log survival is a convex function, which usually results in the assumption that survival greatly increases at low spawner biomass (Fig. 1), is not strongly supported by the data and may be very dangerous for management decisions in extrapolations to low abundance.

Estimation method

Mixed effects models

Our contention is that focusing on one population at a time can be misleading. In this section, we shall demonstrate how this can be avoided by incorporating the estimation of the Ricker model into a standard linear mixed model. Parameter estimation is easy using widely available software, e.g. SAS or S-PLUS.

We will change the notation slightly to put the results in the standard notation of variance components and mixed models. We consider p populations, subscripted by i , for each of which we want to estimate the parameters of a Ricker model (eq. 4) of the form

$$(8) \quad \log \frac{R_{i,t}}{S_{i,t}} = \log \tilde{\alpha}_i + \beta_i S_{i,t} + \varepsilon_{it}$$

where $R_{i,t}$ is recruitment to year-class t in population i , $S_{i,t}$ is spawner abundance in year t in population i , $\tilde{\alpha}_i$ and β_i are the Ricker model parameters for population i , and ε_{it} is estimation error, assumed normal. We assume that $\log \tilde{\alpha}_i$ is a normal random variable and define $\mu + a_i \equiv \log \tilde{\alpha}_i$, where μ is the mean of the log-transformed maximum annual reproductive rates and a_i is the random effect for population i . (Note that we will repeat the above calculations using the lifetime reproductive rate instead of the annual reproductive rate.)

We consider the log survival, $\log(R/S)$, of a year-class from a given population as an element of a vector \mathbf{y} . If there are n_i observations for population i , then the first n_1 elements of the vector \mathbf{y} will be the n_1 log survivals for the first population, followed by the n_2 log survivals for the second population, and so on.

We consider the fixed effects of the model first. The parameters that we estimate are the overall mean, μ , and p regression parameters, β_i . We consider the spawner abundances, $S_{i,t}$, as known and estimate the density-dependent regression parameter β_i for each population. The standard mixed model notation for the vector of fixed effects parameters is β . The unknown vector β consists of the overall mean μ and the $p\beta_i$ s. The vector β is related to \mathbf{y} by the known model matrix \mathbf{X} , whose elements are 0, 1, and $S_{i,t}$; the form of this matrix is given below.

For the vector of random effects composed of the a_i , we shall use the standard mixed model notation \mathbf{u} . The vector \mathbf{u}

is related to \mathbf{y} by a known model matrix \mathbf{Z} whose form is given below.

In standard mixed model notation, we have

$$(9) \quad \mathbf{y} = \mathbf{X}\beta + \mathbf{Z}\mathbf{u} + \boldsymbol{\varepsilon}.$$

Here, $\boldsymbol{\varepsilon}$ is an unknown random error vector. For example, consider the simple case of two populations, each of which is observed for 3 years with the first year denoted by 1. The above equation can then be written as

$$(10) \quad \mathbf{y} = \begin{bmatrix} y_{11} \\ y_{12} \\ y_{13} \\ y_{21} \\ y_{22} \\ y_{23} \end{bmatrix} = \begin{bmatrix} 1 & S_{11} & \cdot \\ 1 & S_{12} & \cdot \\ 1 & S_{13} & \cdot \\ 1 & \cdot & S_{21} \\ 1 & \cdot & S_{22} \\ 1 & \cdot & S_{23} \end{bmatrix} \begin{bmatrix} \mu \\ \beta_1 \\ \beta_2 \end{bmatrix} + \begin{bmatrix} 1 & \cdot \\ 1 & \cdot \\ 1 & \cdot \\ 1 & \cdot \\ \cdot & 1 \\ \cdot & 1 \end{bmatrix} \begin{bmatrix} a_1 \\ a_2 \end{bmatrix} + \begin{bmatrix} \varepsilon_{11} \\ \varepsilon_{12} \\ \varepsilon_{13} \\ \varepsilon_{21} \\ \varepsilon_{22} \\ \varepsilon_{23} \end{bmatrix}$$

where $y_{i,t} = \log(R_{i,t}/S_{i,t})$. The generalization provided by the mixed model enables one not only to model the mean of \mathbf{y} (as in the standard linear model), but to model the variance of \mathbf{y} as well. We assume that \mathbf{u} and $\boldsymbol{\varepsilon}$ are uncorrelated and have multivariate normal distributions with expectations $\mathbf{0}$ and variances \mathbf{D} and \mathbf{R} , respectively. The variance of \mathbf{y} is thus

$$(11) \quad \mathbf{V} = \mathbf{Z}\mathbf{D}\mathbf{Z}' + \mathbf{R}.$$

One can model the variance of the data, \mathbf{y} , by specifying the structure of \mathbf{D} and \mathbf{R} . We assume that $\mathbf{D} = \sigma_d^2 \mathbf{I}$ (where \mathbf{I} is the identity matrix), i.e., that the variability among populations of $\log \tilde{\alpha}_i$ is normally distributed with variance σ_d^2 . In the simplest case, one might assume that the error variance is the same for all populations, i.e., $\mathbf{R} = \sigma^2 \mathbf{I}$. (Note that when $\mathbf{R} = \sigma^2 \mathbf{I}$ and $\mathbf{Z} = \mathbf{0}$, the mixed model reduces to the standard linear model.) However, we estimate a separate estimation error variance, σ_i^2 , for each population. We also test whether the residuals are autocorrelated. If they are, we can estimate a separate autocorrelation parameter, ρ_i , for each population. This results in a block diagonal structure for \mathbf{R} , with blocks

$$(12) \quad \sigma_i^2 \begin{bmatrix} 1 & \rho_i & \rho_i^2 & \dots \\ \rho_i & 1 & \rho_i & \dots \\ \rho_i^2 & \rho_i & 1 & \dots \\ \vdots & \vdots & \vdots & \ddots \end{bmatrix}.$$

Estimation of variance components

Now that we have transformed the problem into this form, estimation is trivial because high-quality software exists for this problem (Appendix 1). The likelihood function for the data vector $\mathbf{y} \sim \mathcal{N}_N(\mathbf{X}\beta, \mathbf{V})$ is

$$(13) \quad L = L(\beta, \mathbf{V} | \mathbf{y}) = \frac{e^{-\frac{1}{2}(\mathbf{y}-\mathbf{X}\beta)' \mathbf{V}^{-1} (\mathbf{y}-\mathbf{X}\beta)}}{(2\pi)^{\frac{N}{2}} |\mathbf{V}|^{\frac{1}{2}}}$$

where N is the number of fixed effects estimated, i.e., $N = 1 + p$. There are two common approaches to the estimation of variance components based on this function: maximum likelihood (ML) and restricted maximum likelihood (REML) (Searle et al. 1992). REML differs from ML for this model in that it takes into account the degrees of freedom used for estimating the fixed effects, whereas ML does not. Furthermore, in the case of balanced data, REML solutions are identical to ANOVA estimators, which have known optimality properties. For these reasons, we will use REML but will consider ML to check sensitivity. Denote the resulting estimates of \mathbf{D} and \mathbf{R} by $\hat{\mathbf{D}}$ and $\hat{\mathbf{R}}$, respectively.

It is possible for the estimate of the variance among populations, $\hat{\sigma}_a^2$, to be zero. This often occurs when only a few populations are available for analysis and should not be interpreted as implying that there is no variability among populations in the maximum annual reproductive rate.

Estimation of individual population parameters

The use of mixed models allows us to obtain improved estimates of parameters for any one population. In general, we wish not only to estimate the fixed model parameters, but also to predict the random variables for each population. In our case, we wish to estimate the density-dependent parameter β and predict the slope at the origin for each population, which is assumed to be a random variable. The terminological distinction between estimation of fixed effects and prediction of random effects is awkward and unnecessary (Robinson 1991); we will "estimate" both fixed and random effects, with the understanding that for random effects, we are in fact obtaining estimates of their realized values.

The best linear unbiased estimators (BLUEs) $\hat{\beta}$ of the fixed effects β and the best linear unbiased predictors (BLUPs) $\hat{\mathbf{u}}$ of the random effects \mathbf{u} may be obtained from the mixed model equations

$$(14) \quad \begin{bmatrix} \mathbf{X}' \mathbf{R}^{-1} \mathbf{X} & \mathbf{X}' \mathbf{R}^{-1} \mathbf{Z} \\ \mathbf{Z}' \mathbf{R}^{-1} \mathbf{X} & \mathbf{Z}' \mathbf{R}^{-1} \mathbf{Z} + \mathbf{D}^{-1} \end{bmatrix} \begin{bmatrix} \hat{\beta} \\ \hat{\mathbf{u}} \end{bmatrix} = \begin{bmatrix} \mathbf{X}' \mathbf{R}^{-1} \mathbf{y} \\ \mathbf{Z}' \mathbf{R}^{-1} \mathbf{y} \end{bmatrix}.$$

Without the \mathbf{D}^{-1} in the lower right-hand submatrix of the matrix on the left, eq. 14 would be the ML equations for the model treated as if \mathbf{u} represented fixed effects, rather than random effects. Although the above equation has been discussed in terms of classical methods, the same result is arrived at using a formal Bayes analysis of incorporating prior information into the analysis of data (Searle et al. 1992).

Since we do not know the variance-covariance matrices \mathbf{D} and \mathbf{R} , we substitute $\hat{\mathbf{D}}$ and $\hat{\mathbf{R}}$ into eq. 14 to obtain empirical BLUEs and BLUPs.

The variance-covariance matrix for $[\hat{\beta} \ \hat{\mathbf{u}}]'$ is

$$(15) \quad \mathbf{C} = \begin{bmatrix} \mathbf{X}' \mathbf{R}^{-1} \mathbf{X} & \mathbf{X}' \mathbf{R}^{-1} \mathbf{Z} \\ \mathbf{Z}' \mathbf{R}^{-1} \mathbf{X} & \mathbf{Z}' \mathbf{R}^{-1} \mathbf{Z} + \mathbf{D}^{-1} \end{bmatrix}^-$$

where the superscript minus on the above matrix represents a generalized inverse. An approximate variance-covariance matrix $\hat{\mathbf{C}}$ may be obtained by substituting $\hat{\mathbf{D}}$ and $\hat{\mathbf{R}}$ into eq. 15. The approximate standard error for any linear combination \mathbf{L} of the vector $[\hat{\beta} \ \hat{\mathbf{u}}]'$ may be obtained from

$$(16) \quad \sqrt{\mathbf{L}' \hat{\mathbf{C}} \mathbf{L}} .$$

Note that these standard errors will tend to be underestimates of the standard errors of the empirical BLUPs and BLUEs (Searle et al. 1992).

Our estimation methods above provide estimates of μ for each species and (the realized values of) the a_i . As long as the log-transformed values are considered, the interpretation is simple; however, the interpretation of the values on an untransformed scale is more complex. For a species, the median $\tilde{\alpha}$ is $\exp(\mu)$, and the expectation is $\exp(\mu + 0.5\sigma_a^2)$, where the expectation and median are taken with respect to the distribution of the random effects. This estimate is complicated by the estimation error of the μ and the σ_a^2 , which we will ignore here. To keep things simple, we will discuss our results in terms of the log-transformed values and the medians of $\tilde{\alpha}$ for a species, except where noted.

Data sources and treatment

The data that we used are estimates obtained from assessments compiled by Myers et al. (1995). The database is available from the first author. For marine populations, population numbers and fishing mortality were usually estimated using sequential population analysis (SPA) of commercial and (or) recreational catch at age data for most marine populations. SPA techniques include virtual population analysis (VPA), cohort analysis, and related methods that reconstruct population size from catch at age data (see Hilborn and Walters (1992, chaps. 10 and 11) for a description of the methods used to reconstruct the population history). Briefly, the catch at age is combined with estimates from research surveys and (or) commercial catch rates to estimate the numbers at age in the final year and to reconstruct previous numbers at age under the assumption that catch at age is known without error and that natural mortality at age is known and constant.

For salmon stocks, spawner abundance is the estimate of the number of fish reaching the spawning grounds, and recruitment is estimated by combining catch and the number of upstream migrants.

SPA techniques were used for the freshwater species except for brook trout (*Salvelinus fontinalis*). The brook trout populations were from introduced populations in California mountain lakes (DeGisi 1994); these populations were estimated using research gill nets and ML depletion estimation.

Time series of less than 10 paired spawner-recruit observations are not included in this analysis. The $SPR_{F=0}$ was calculated using estimates of natural mortality, weight at age, and maturity at age. Maturity and weight at age were usually estimated from research surveys carried out for each population.

A major source of uncertainty in the SPA estimates of recruitment and spawning stock biomass (SSB) is that they usually assume that catches are known without error. This is particularly important when estimates of discarding and mis-reporting are not included in the catch at age data used in the SPA. These errors are clearly important for some periods of time for some of the cod stocks (Myers et al. 1997a), and these errors will affect our estimates of the number of replacements that each spawner can produce at low population densities ($\tilde{\alpha}$).

The data for this analysis are available at R.A. Myers' web site (<http://fish.dal.ca/welcome.html>).

Results

We first used ML for a standard Ricker model to obtain single-population estimates of $\log \tilde{\alpha}$ for each population (Fig. 3). Then, for each species in our database, we applied the mixed model to the data from all of the populations belonging to that species, obtaining estimates and predictions as follows. We used REML to estimate σ_a^2 , the true variability among populations in the log-transformed maximum annual reproductive rate, and for each population, σ_i^2 , the estimation error variance. These estimated variance components were then used to obtain the empirical BLUE of the mean log-transformed maximum annual reproductive rate, μ , for the species and the empirical BLUP of $\log \tilde{\alpha}$ for each population (Table 1). For completeness, we have given the mixed model estimates for the mean and variability at the family level; however, they should be used with great caution because they may not be representative of any given species. More detailed results (which include stock-level estimates) are available at R.A. Myers' web site.

Note that there is less variance among the BLUP estimates than among the single-population estimates (Fig. 4).

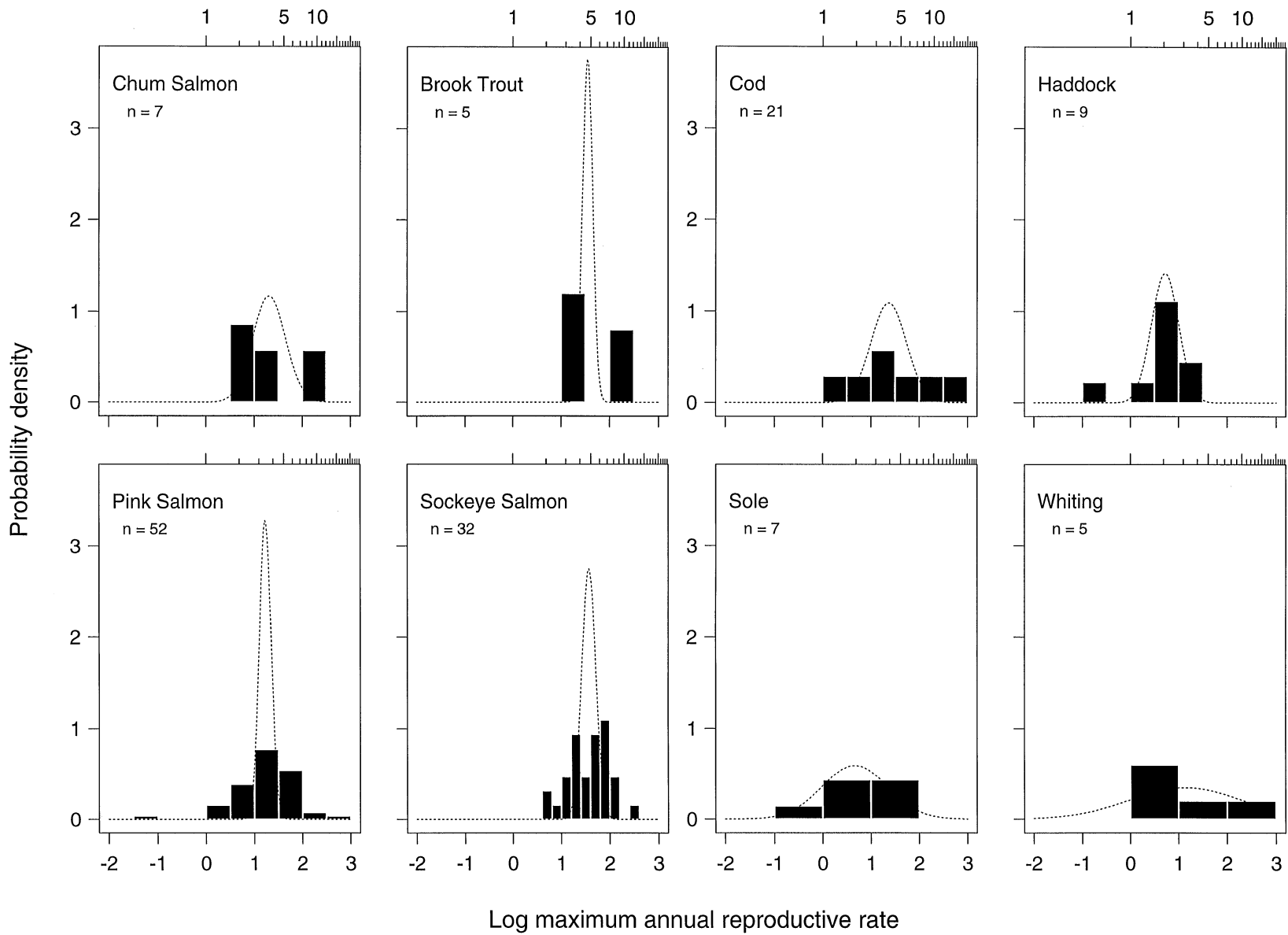
The estimates for populations with large estimation error variances (e.g., due to relatively few data points) and that are far from the mean for the species, e.g. Gulf of Maine cod (MLE: $\log \tilde{\alpha} = 2.85$, BLUP: $\log \tilde{\alpha} = 1.84$), are pulled towards the mean more than those for populations with lower estimation error variance and that are close to the species mean, e.g. Iceland cod (MLE: $\log \tilde{\alpha} = 1.19$, BLUP: $\log \tilde{\alpha} = 1.19$).

As expected, the estimate of the true variability in the maximum annual reproductive rate is much less than the sample variability because individual estimates contain estimation error. For example, for pink salmon, if $\tilde{\alpha}$ is estimated separately for each stock, then there is an order of magnitude range of the estimates. However, if $\tilde{\alpha}$ is assumed to be a random variable, then the mixed model estimates suggest that the true range is very small, with all the true values being very close to 3 (Fig. 3). Cod show a similar picture. The median number of replacement spawners per spawner per year for cod at low abundance is between 3 and 4, resulting in a maximum net reproductive rate (if there is no fishing mortality) of between 15 and 20. The maximum annual reproductive rate for Atlantic herring (*Clupea harengus*) appears to be slightly less, and for hakes of the genus *Merluccius*, e.g., silver hake (*Merluccius bilinearis*) and Pacific hake (*Merluccius productus*), it is around 1. Some anadromous species, e.g., sockeye salmon (*Oncorhynchus nerka*), appear to have a maximum annual reproductive rate of around 4 or 5, while others, e.g., pink salmon, have a much lower rate.

The most remarkable aspect of the results is the relative constancy of the estimates of the maximum annual reproductive rate. For species for which we have more than one population in our analysis, the median of the estimated maximum reproductive rate is almost always between 1 and 7 (Fig. 5a).

For the species with multiple populations, only Pacific ocean perch (*Sebastodes alutus*) and silver hake have an esti-

Fig. 3. Histograms by species of the individual ML estimates of the log of the maximum annual reproductive rate, $\log \tilde{\alpha}$, compared with probability densities based on REML estimates of the true variability in $\log \tilde{\alpha}$ from our mixed model analysis (dotted line). Note that the top axis of each plot shows the untransformed annual reproductive rate. The number of populations (n) for each histogram is also given.



mated maximum annual reproductive rate of less than 1. The low estimate for Pacific ocean perch results in a very low estimate for the expected maximum lifetime reproductive rate, i.e., it is about 3 (Table 1; Fig. 6a). Relatively low estimates of the maximum lifetime annual reproductive rate and steepness were estimated for the other *Sebastodes* species (Table 1). We do not know whether these low estimates are real, e.g., are somehow related to their low natural mortality and oviparous reproduction, or an artifact. The age-based assessments of the *Sebastodes* species are unusually uncertain because of aging difficulties. It is also possible that the environmental conditions in recent years, when the low estimates of spawning biomass and recruitment were made, have been unusual and have resulted in lower than average estimates. In any case, it is crucial to determine if the assessments are correct and exploit these species more cautiously than other species.

The estimates of the maximum annual reproductive rate for species for which we have only one population are much more variable than for the species with many populations (Figs. 5b and 6b). The greater variability in these estimates is at least partially caused by estimation error. However, several species have maximum reproductive rates that suggest that they cannot sustain intense fisheries. In some cases, this is certainly true. The southern bluefin tuna (*Thunnus maccoyii*) in the Southern Ocean has been greatly reduced by overfishing. In other cases, there may be serious problems with the assessments.

Despite the large variation in the individual estimates, our general conclusion about the relative constancy of the maximum annual reproductive rate stands; the estimates are usually around 3. There are exceptions for individual stocks, but these usually have large standard errors.

Note that herring has a smaller maximum reproductive rate than many species. The lower mean is due to a few stocks in the northern North Atlantic that have been reduced to very low levels (the Iceland stocks, the Norway stock (often called the "Arcto-Norwegian" stock), and the Georges Bank stocks).

We also considered a model that allowed the residuals to be autocorrelated (see Appendix 1 for the computer code used in the estimation). This approach is probably preferable if autocorrelation is substantial in the model residuals, but may pull the individual estimates too far towards the population mean.

We repeated the above analysis for the lifetime maximum reproductive rate and display the results in terms of the expected lifetime maximum reproductive rate and the steepness. Among taxonomic groups, the lifetime reproductive rate appears to be more variable than the annual rate; however, for species with similar natural mortalities after reproduction, the results are again relatively constant.

The results for the steepness are displayed as the median, the 20th percentiles, and the 80th percentiles (Table 1). These can be used to approximate priors for Bayesian analyses that commonly use steepness (Punt and Hilborn 1997).

It is useful to compare the median for a species of the maximum annual reproductive rate (the uncorrected value) with the expectation, where the median and expectation are taken with respect to the distribution of the random effects

(Fig. 7). The corrected estimates are higher by a factor of $\exp(0.5\sigma_a^2)$. This effect is usually small except for species where the estimate of the variability among populations is unusually large, e.g., for blueback herring (*Alosa aestivalis*).

A generalization

The unexpected generalization that comes from our analysis is that the annual reproductive rate within a species often shows relatively little variation and that the variation in annual reproductive rate among species is surprisingly small, usually ranging from 1 to 7 for species for which we have several populations represented in our analysis.

This is a broad generalization that may have great implications for the management and conservation of fish populations. Although the generalization appears to be firmly established for many well-studied species, these are primarily temperate-zone species.

Possible exceptions

In this section, we will discuss several populations that appear to have anomalously high or low annual reproductive rates. It is unclear whether these rates are real or due to limitations in the assessments.

The blueback herring appears to have a relatively high maximum annual reproductive rate. This relatively high number is consistent with the fast growth rate experienced by this species and other *Alosa* species when they recolonize former habitat (Crecco and Gibson 1990). However, it is possible that these high rates of population growth are caused by movement of fish upstream over obstructions and not population growth per se. This hypothesis needs to be evaluated.

Chinook salmon (*Oncorhynchus tshawytscha*) also appears to have relatively high maximum annual reproductive rates. These appear to be real and are probably conservative. The values that are in the figures for chinook salmon are from the northern limit of the range. The values for the Columbia River appear to be much higher, but it is impossible to estimate the "natural" rates because of dam-induced mortality.

The ayu (*Plecoglossus altivelis*, Plecoglossidae, Salmoniformes) from Lake Biwa, Japan, is the only univoltine species in the database, and it appears to have a very high annual reproductive rate (Table 1) (Suzuki and Kitahara 1996). The analysis appears to be sound and is backed up by fishery-independent survey data, but it is possible that the application of VPA for this species may have led to biases.

Among the lowest estimates of the maximum reproductive rates are those for several species on the west coast of North America: Pacific ocean perch, sablefish (*Anoplopoma fimbria*), and chilipepper rockfish (*Sebastodes goodei*). These stocks all are assessed in a similar manner. The assessments on these stocks do not have reliable fishery-independent estimates of abundance, do not have a large amount of aging data, and often assume that the population is at the unfished equilibrium at the beginning of the fishery. It is critical for the management of these stocks to determine whether their actual maximum reproductive rate is as low as it appears to be, or if the assessments are reliable.

These cases represent anomalies, which may represent fundamental inconsistencies with our broad generalization about the reproductive rate, or may well be explained by

Table 1. Mixed model estimates at the species and family levels and corresponding estimates of the percentiles of z (the steepness parameter).

Species	<i>n</i>	$\widehat{\log \alpha}$	SE	$\hat{\sigma}_a^2$	$\hat{\alpha}$	z_{20}	z_{med}	z_{80}
Aulopiformes								
Synodontidae	1	0.31	0.07		2		0.34	
Bombay duck (<i>Harpodon nehereus</i>)	1	0.31	0.07		2		0.34	
Clupeiformes								
Clupeidae	34	1.06	0.19	1.16	17.1	0.49	0.71	0.86
Anadromous alewife (<i>Alosa pseudoharengus</i>)	4	1.29	0.09	0	5.7		0.59	
Anadromous American shad (<i>Alosa sapidissima</i>)	1	1.65	0.3		18.5		0.82	
Atlantic menhaden (<i>Brevoortia tyrannus</i>)	1	2.2	0.12		24.8		0.86	
Blueback herring (<i>Alosa aestivalis</i>)	3	2.6	0.55	0.81	31.9	0.71	0.84	0.92
Gulf menhaden (<i>Brevoortia patronus</i>)	1	1.25	0.16		5.3		0.57	
Atlantic herring (<i>Clupea harengus</i>)	18	0.73	0.28	1.31	22.1	0.52	0.74	0.88
Pacific sardine (<i>Sardinops sagax</i>)	2	0.66	0.89	1.56	12.7	0.34	0.59	0.81
Spanish sardine (<i>Sardina pilchardus</i>)	1	-0.56	0.75		2.1		0.34	
Sprat (<i>Sprattus sprattus</i>)	3	0.87	0.55	0.71	10.7	0.48	0.65	0.79
Engraulidae	4	1.28	0.57	1.14	11.5	0.4	0.62	0.8
Anchovy (<i>Engraulis encrasicolus</i>)	2	0.7	0.13	0	3.6		0.47	
Gold-spotted grenadier anchovy (<i>Coilia dussumieri</i>)	1	2.73	0.19		17.6		0.81	
Northern anchovy (<i>Engraulis mordax</i>)	1	0.33	0.41		3.1		0.43	
Gadiformes								
Gadidae	49	1.01	0.12	0.51	19.6	0.67	0.79	0.87
Blue whiting (<i>Micromesistius poutassou</i>)	2	0.59	0.33	0	10		0.71	
Atlantic cod (<i>Gadus morhua</i>)	21	1.37	0.15	0.37	26	0.76	0.84	0.9
Haddock (<i>Melanogrammus aeglefinus</i>)	9	0.72	0.21	0.28	13	0.64	0.74	0.82
Hake (<i>Merluccius hubbsi</i>)	1	1.18	0.45		18		0.82	
Pacific hake (<i>Merluccius productus</i>)	1	-0.95	0.83		1.9		0.32	
Pollock or saithe (<i>Pollachius virens</i>)	5	1.16	0.14	0.05	18	0.78	0.81	0.84
Silver hake (<i>Merluccius bilinearis</i>)	3	-0.18	0.29	0.16	2.7	0.31	0.39	0.47
Walleye pollock (<i>Theragra chalcogramma</i>)	2	0.28	0.24	0.01	5	0.53	0.55	0.58
Whiting (<i>Merlangius merlangus</i>)	5	1.14	0.51	1.16	30.8	0.64	0.81	0.91
Lophiiformes								
Lophiidae	1	-0.07	0.32		6.7		0.64	
Black anglerfish (<i>Lophius budegassa</i>)	1	-0.07	0.32		6.7		0.63	
Perciformes								
Carangidae	3	0.27	0.21	0	4		0.5	
Horse mackerel (<i>Trachurus trachurus</i>)	2	0.52	0.8	0	12.1		0.75	
Mediterranean horse mackerel (<i>Trachurus mediterraneus</i>)	1	0.25	0.22		3.5		0.47	
Lutjanidae	1	1.9	0.9		47.8		0.95	
Red snapper (<i>Lutjanus campechanus</i>)	1	1.9	0.9		47.8		0.92	
Percichthyidae	1	0.95	0.16		18.6		0.82	
Striped bass (<i>Morone saxatilis</i>)	1	0.95	0.16		18.6		0.82	
Percidae	2	0.91	0.57	0.28	9.5	0.57	0.67	0.76
Walleye (<i>Stizostedion vitreum</i>)	2	0.91	0.57	0.28	9.5	0.57	0.67	0.76
Scianidae	1	1.88	0.28		26.1		0.87	
White croaker (<i>Argyrosomus argentatus</i>)	1	1.88	0.28		26.1		0.87	
Scombridae	8	0.34	0.39	1.12	7.5	0.3	0.52	0.72
Atlantic bluefin tuna (<i>Thunnus thynnus</i>)	1	-0.4	0.23		5.2		0.56	
Bigeye tuna (<i>Thunnus obesus</i>)	2	0.73	0.08	0	5.3		0.57	
Chub mackerel (<i>Scomber japonicus</i>)	1	-0.05	0.33		2.4		0.38	
Atlantic mackerel (<i>Scomber scombrus</i>)	2	1.11	0.91	1.29	31.8	0.62	0.81	0.92
Southern bluefin tuna (<i>Thunnus maccoyii</i>)	1	-1.5	0.09		2.9		0.42	
Yellowfin tuna (<i>Thunnus albacares</i>)	1	1.43	0.21		9.3		0.7	
Sparidae	3	2.48	0.41	0	65.9		0.95	
New Zealand snapper (<i>Pagrus auratus</i>)	2	1.34	1.31	0	65.6		0.94	
Scup (<i>Stenotomus chrysops</i>)	1	2.6	0.38		74.6		0.95	

Table 1 (concluded).

Species	<i>n</i>	$\widehat{\log \alpha}$	SE	$\hat{\sigma}_a^2$	$\hat{\alpha}$	z_{20}	z_{med}	z_{80}
Xiphiidae	1	1.7	0.05		30.1		0.88	
Swordfish (<i>Xiphias gladius</i>)	1	1.7	0.05		30.1		0.88	
Pleuronectiformes								
Pleuronectidae	14	0.79	0.18	0.34	18.8	0.71	0.8	0.87
European flounder (<i>Platichthys flesus</i>)	1	-0.03	0.42		5.3		0.57	
Greenland halibut (<i>Reinhardtius hippoglossoides</i>)	3	0.75	0.68	1.32	29.3	0.59	0.79	0.91
Plaice (<i>Pleuronectes platessa</i>)	8	0.92	0.17	0.08	25.1	0.83	0.86	0.88
Yellowtail flounder (<i>Pleuronectes ferrugineus</i>)	2	0.79	0.34	0.14	13	0.69	0.75	0.81
Soleidae	7	0.66	0.35	0.68	28.7	0.72	0.84	0.91
Sole (<i>Solea vulgaris</i>)	7	0.66	0.35	0.68	28.7	0.72	0.84	0.91
Salmoniformes								
Esocidae	2	0.51	0.19	0.03	6.1	0.57	0.6	0.64
Northern pike (<i>Esox lucius</i>)	2	0.51	0.19	0.03	6.1	0.57	0.6	0.64
Plecoglossidae	1	4.73	0.16		123.5		0.97	
Ayu (<i>Plecoglossus altivelis</i>)	1	4.73	0.16		123.5		0.97	
Salmonidae	106	1.43	0.05	0.18	25.1	0.8	0.85	0.89
Atlantic salmon (<i>Salmo salar</i>)	3	1.46	0.25	0.16	5.1	0.46	0.54	0.62
Chinook salmon (<i>Oncorhynchus tshawytscha</i>)	6	1.99	0.13	0	7.3		0.65	
Chum salmon (<i>Oncorhynchus keta</i>)	7	1.31	0.24	0.34	4.4	0.36	0.48	0.6
Freshwater brook trout (<i>Salvelinus fontinalis</i>)	5	1.55	0.24	0.11	27.4	0.83	0.87	0.89
Lake trout (<i>Salvelinus namaycush</i>)	1	0.92	0.08		24.1		0.86	
Pink salmon (<i>Oncorhynchus gorbuscha</i>)	52	1.22	0.07	0.12	3.6	0.39	0.46	0.53
Sockeye salmon (<i>Oncorhynchus nerka</i>)	32	1.57	0.08	0.15	5.2	0.47	0.55	0.62
Scorpaeniformes								
Anoplopomatidae	1	-2.35	0.47		1.4		0.28	
Sablefish (<i>Anoplopoma fimbria</i>)	1	-2.35	0.47		1.4		0.26	
Hexagrammidae	1	1.13	0.49		12		0.77	
Atka mackerel (<i>Pleurogrammus monopterygius</i>)	1	1.13	0.49		12		0.75	
Scorpaenidae	5	-1.57	0.24	0.17	2.8	0.31	0.39	0.48
Chilipepper (<i>Sebastes goodei</i>)	1	-0.85	0.57		2.1		0.35	
Pacific ocean perch (<i>Sebastes alutus</i>)	3	-1.93	0.18	0	3		0.43	
Deepwater redfish (<i>Sebastes mentella</i>)	1	-1.08	0.18		3.6		0.47	

Note: Listed are the empirical BLUE of the mean value of the log-transformed maximum annual reproductive rate ($\widehat{\log \alpha}$), its standard error, the estimated variance among populations ($\hat{\sigma}_a^2$) (where possible), the estimated expected maximum lifetime reproductive rate for a species, where the expectation is taken over the distribution of the random effects ($\hat{\alpha}$), the 20th percentile of z (z_{20}) (where possible), the median of z (z_{med}), and the 80th percentile of z (z_{80}) (where possible). The mixed model estimates are given at the species and family levels, but the family-level estimates (shown in boldface) should be used with caution.

other factors, e.g., assessment problems or the possibility that the data for these species come from only a relatively short time period, which may not be representative of the average reproductive rate.

Limitations and alternative approaches

Our approach to estimating the standardized slope at the origin of spawner–recruit functions is based on well-studied statistical methods and has intuitive appeal and appears to be a promising method for categorizing species in terms of their vulnerability to overfishing. However, researchers should be aware of its limitations and of alternative approaches.

The first limitation is the functional form assumed for density-dependent mortality. The Ricker model and the non-linear Ricker model (eq. 6) are not appropriate for some species. This is a serious limitation of the methods described here. For example, we did not consider coho salmon (*Oncorhynchus kisutch*) in this analysis because the shape of the spawner–recruitment curve was clearly asymptotic, simi-

Fig. 4. Comparison of the maximum annual reproductive rate, $\log \hat{\alpha}$, obtained from individual regressions on each cod population in the North Atlantic with the empirical BLUPs obtained from a mixed model analysis. Notice that the mixed model estimates have lower variance than the individual estimates.

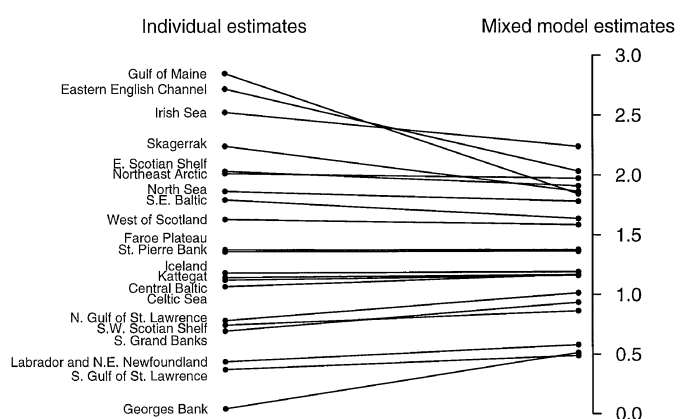
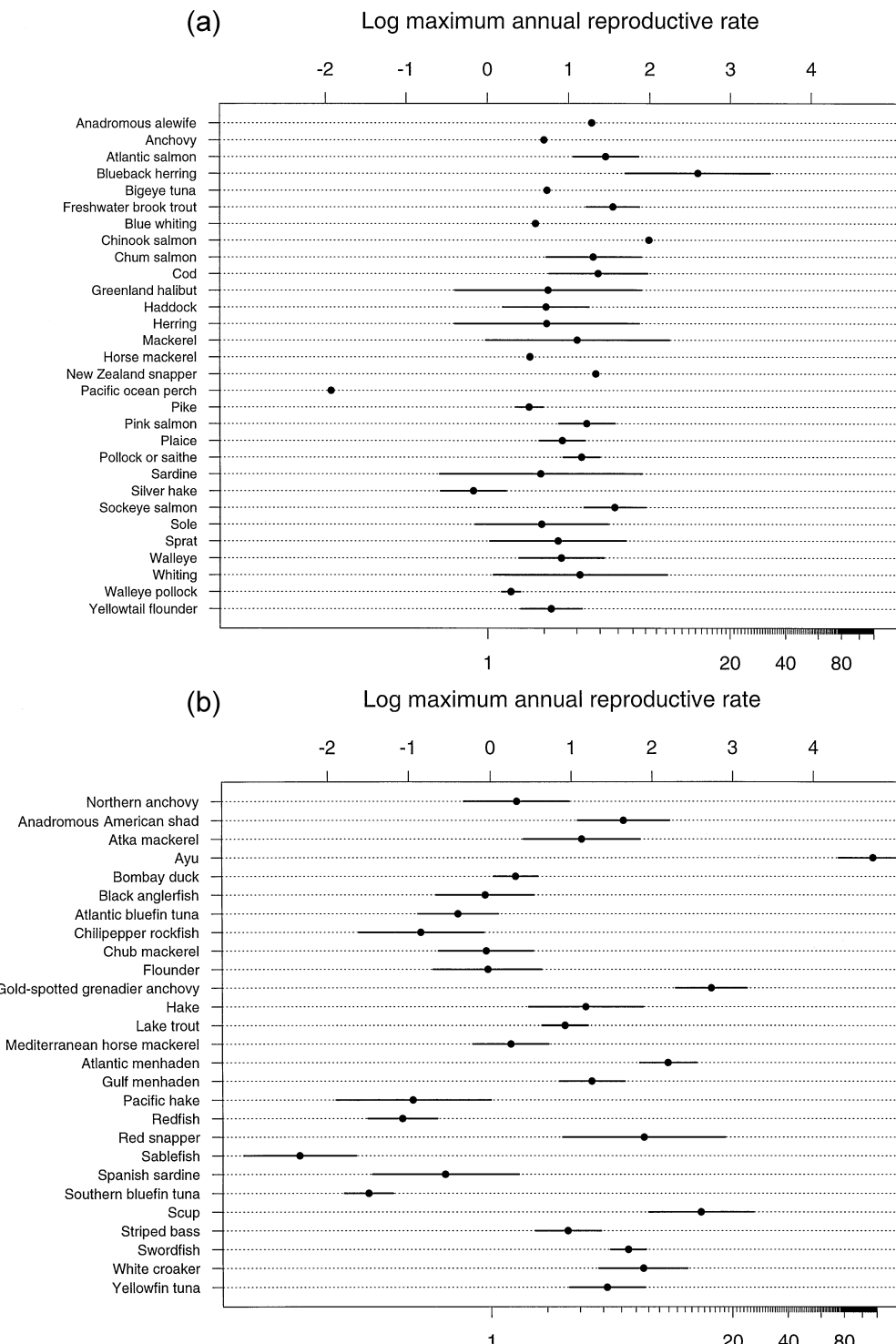


Fig. 5. Estimates of the log of the maximum annual reproductive rate for (a) species with multiple populations in the database, where the error bars represent the estimated standard deviation of the log of the maximum annual reproductive rate (this estimate is sometimes zero if only two or three populations are used in the analysis), and (b) species with only one population in the database, where the error bars represent the standard error of the estimate.



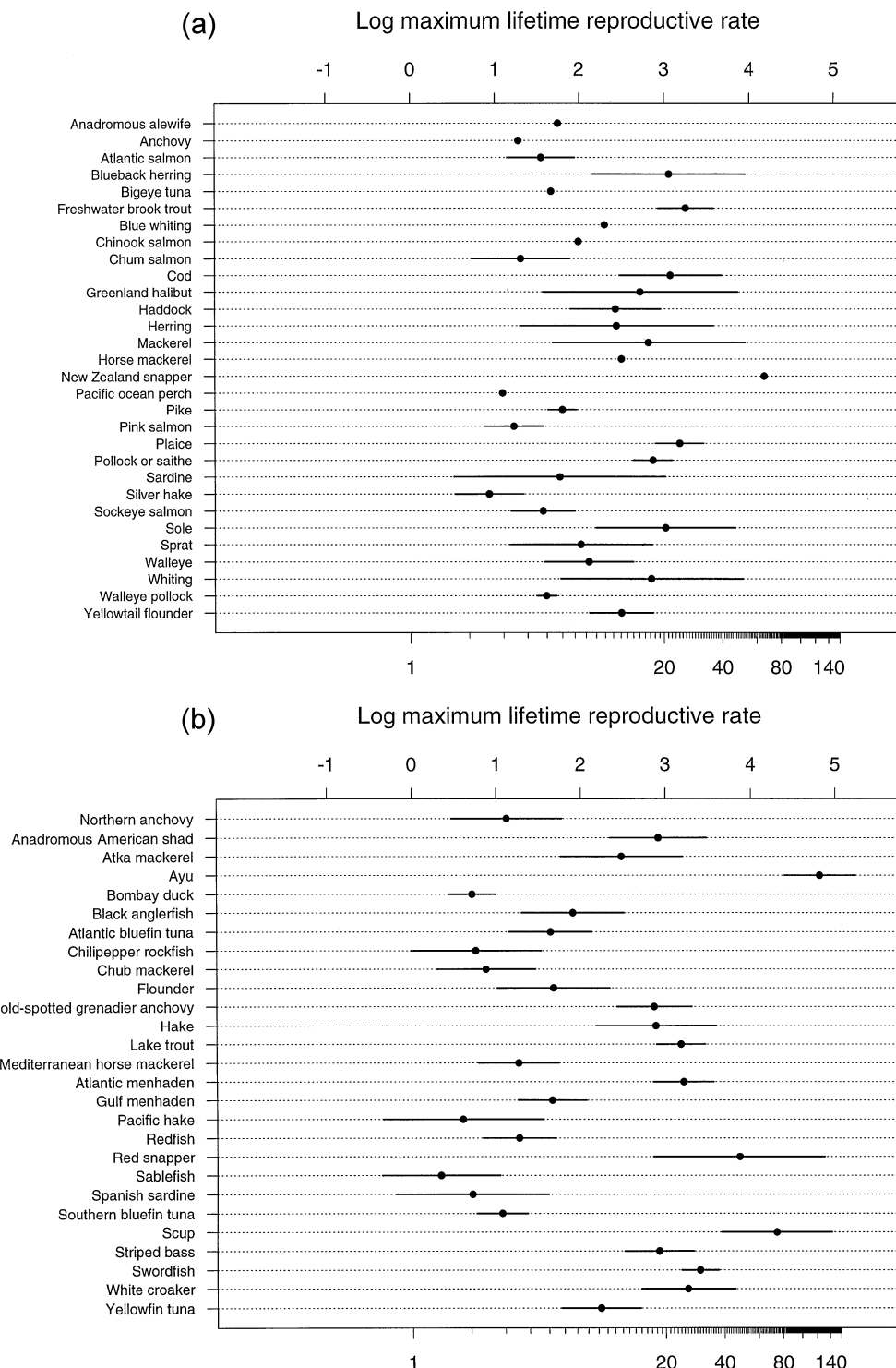
lar to a Beverton–Holt function. For such functions, nonlinear mixed models are required and will be considered in a future paper using the methods of Lindstrom and Bates (1990).

The second limitation is that we have assumed that the distribution of α is approximately lognormal. This appears

to be a reasonable approximation in most cases considered here, but violations of the assumption may cause biases (Verbeke and Lesaffre 1996).

A third limitation is the assumption that the recruitment distribution for given spawner abundance is lognormal. This

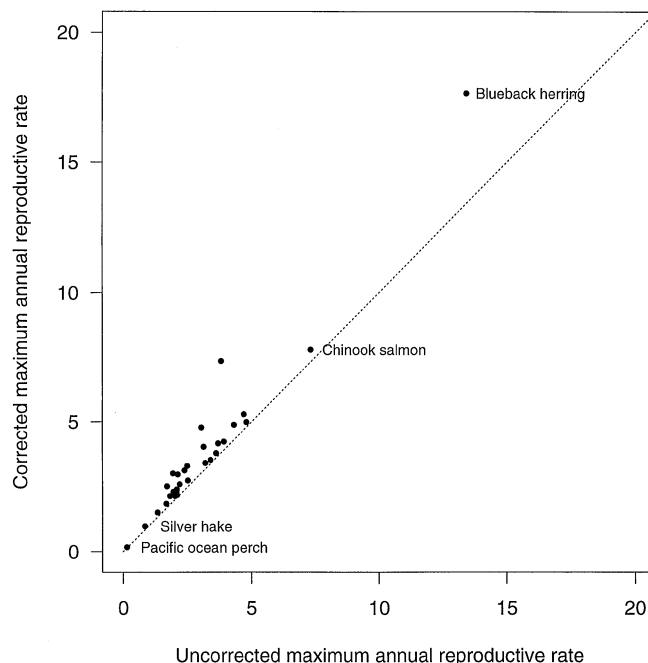
Fig. 6. Estimates of the log of the maximum lifetime reproductive rate for (a) species with multiple populations in the database, where the error bars represent the estimated standard deviation of the log of the maximum lifetime reproductive rate, and (b) species with only one population in the database, where the error bars represent the standard error of the estimate.



is by far the most common assumption used in fitting spawner–recruitment models (Hilborn and Walters 1992); however, it may not always be the most appropriate assumption. The gamma distribution appears to give more reasonable fits to some stock–recruitment data (Myers et al. 1995; R.A. Myers, K.G. Bowen, and I.A. Zouros, unpublished data).

A fourth limitation is the assumption that all populations within a taxon are comparable, i.e., the maximum reproductive rate for populations within a species (or higher taxon) is described by a lognormal distribution. It is possible that this parameter may vary in a systematic way among populations, e.g., populations in colder conditions may have a lower max-

Fig. 7. Comparison of the uncorrected (simple exponential transform) and corrected (lognormal) values for the maximum annual reproductive rate. Notice that without the lognormal correction, the maximum annual reproductive rate will be underestimated.



imum reproductive rate. Such hypotheses can be investigated by letting the maximum reproductive rate be a random variable whose mean is a function of a covariate such as temperature or latitude.

If any of the above four assumptions appears to be violated seriously, then an alternative approach is needed. Perhaps the most convenient alternative framework for this type of model is either a Bayes or empirical Bayes hierarchical approach (Efron 1996). Punt and Hilborn (1997) have recently reviewed these approaches in fisheries management. McAllister (1994) implemented an empirical Bayes approach to estimating a parameter functionally related to the slope at the origin, viz. the steepness parameter, using an earlier version of the database used here.

The ML estimators that we have used to estimate the underlying distribution of annual reproductive rates may result in estimates that are less "heavy tailed" than they should be (Searle et al. 1992; Efron 1996).

It should be remembered that this analysis does not circumvent known biases, e.g., estimation error in spawner abundance and time series bias in the treatment of spawner-recruitment relationships (for a review, see Hilborn and Walters 1992).

Discussion

The analysis presented in this paper suggests a new and unsuspected finding: the maximum annual reproductive rate for any of the species examined is typically between 1 and 7. This number may be less for some species and more for others, but the relative constancy of the annual reproductive rate is an unanticipated, and very important, finding. This analy-

sis is consistent with our preliminary analysis (Myers et al. 1996).

The common belief that there is no relationship between spawner biomass and recruitment is founded on the notion that the maximum reproductive rate for fish is essentially infinite, a belief based on the observation that fecundity of fish is often large and cursory examination of spawner-recruitment plots that often show no strong reduction of recruitment at low spawner abundances over the range of the observations. This erroneous belief is caused by the lack of attention paid to the information content of different data sets (Myers and Barrowman 1996; Myers 1997).

Hypotheses

This broad generalization demands an explanation. First, consider the lower limit of the annual reproductive rate at low abundance. This represents the "average" value that should occur at low abundance. Clearly, if this value is much less than 1, then the population may very well go extinct because the value would probably be below 1 for considerable lengths of time because of variation in the environment.

Why, then, would the annual reproductive rate be bounded at the upper end? A reasonable, but speculative, answer is that a very high value of the reproductive rate would imply an excess of resources that are not exploited. In this case, other competitors would be expected to evolve to exploit these resources.

Reducing uncertainty

The uncertainty of the biological processes underlying the population dynamics of exploited species can be greatly reduced by combining data from many studies. The relative constancy of the maximum reproductive rate allows for simple, broad conclusions to be reached on the management of fish stocks. That the maximum reproductive rate is typically around 1–7 replacement spawners per spawner per year is a powerful tool for the management of fish stocks. It allows the maximum exploitation rate to be estimated quickly (Mace 1994; Myers and Mertz 1998) and the recovery rates of exploited fish populations to be calculated (Myers et al. 1997b).

Many of the crucial parameters needed for fisheries management can be estimated using the maximum reproductive rate analyzed here together with simple approximations (Myers et al. 1997b; Myers and Mertz 1998). For example, the steepness parameter that we compiled is now commonly used in assessments, and our analysis provides reasonable ML estimates that can be used in empirical Bayes assessment procedures. All that is required to use these approximations are data on natural mortality, age at maturity, and the maximum reproductive rate. These approximate formulas will require testing and verification, but this approach should allow progress to be made on critical issues. Thus, even if the maximum reproductive rate is not known for a species, the estimates compiled in this paper allow it to be approximated, or our estimates can be used in forming priors for a Bayesian analysis.

Acknowledgments

We wish to thank the Killam Foundation, the Canadian Foun-

dation for Innovation, and the Natural Sciences and Engineering Research Council of Canada for financial support. We thank Stacey Fowlow for programming assistance. We thank the hundreds of assessment biologists whose hard work made this meta-analysis possible. Special thanks to Pamela Mace whose input was key to developing these ideas. This paper is dedicated to the memory of my (R.A.M.) great friend, Gordon Mertz.

References

- Barnthouse, L.W., Klauda, R.J., Vaughan, D.S., and Kendall, R.L. 1988. Science, law, and the Hudson River power plants: a case study in environmental assessment. *Am. Fish. Soc. Monogr.* **4**.
- Bellows, T.S. 1981. The descriptive properties of some models for density dependence. *J. Anim. Ecol.* **50**: 139–156.
- Cole, L.C. 1954. The population consequences of life history phenomena. *Q. Rev. Biol.* **29**: 103–137.
- Cook, R.M., Sinclair, A., and Stefansson, G. 1997. Potential collapse of North Sea cod stocks. *Nature (Lond.)*, **358**: 521–522.
- Crecco, V.A., and Gibson, M. 1990. Stock assessment of river herring from selected Atlantic coast rivers. Spec. Rep. 19. Atlantic States Marine Fisheries Commission, Washington, D.C.
- DeGisi, J.S. 1994. Year class strength and catchability of mountain lake brook trout. Master's thesis, University of British Columbia, Vancouver, B.C.
- Efron, B. 1996. Empirical Bayes methods for combining likelihoods. *J. Am. Stat. Assoc.* **91**: 538–565.
- Hilborn, R., and Liermann, M. 1998. Standing on the shoulders of giants: learning from experience in fisheries. *Rev. Fish Biol. Fish.* **8**: 1–11.
- Hilborn, R., and Walters, C.J. 1992. Quantitative fisheries stock assessment: choice, dynamics and uncertainty. Chapman and Hall, New York.
- Lande, R., Engen, S., and Saether, B.E. 1997. Optimal harvesting, economic discounting and extinction risk in fluctuating populations. *Nature (Lond.)*, **372**: 88–90.
- Liermann, M., and Hilborn, R. 1997. Depensation in fish stocks: a hierachic Bayesian metaanalysis. *Can. J. Fish. Aquat. Sci.* **54**: 1976–1985.
- Lindstrom, M.J., and Bates, D.M. 1990. Nonlinear mixed effects models for repeated measures data. *Biometrics*, **46**: 673–687.
- Mace, P.M. 1994. Relationships between common biological reference points used as threshold and targets of fisheries management strategies. *Can. J. Fish. Aquat. Sci.* **51**: 110–122.
- Mace, P.M., and Doonan, I.J. 1988. A generalized bioeconomic simulation model for fish population dynamics. *N.Z. Fish. Assess. Res. Doc.* 88/4.
- Maynard Smith, J., and Slatkin, M. 1973. The stability of predator-prey systems. *Ecology*, **54**: 384–384.
- McAllister, M.K., Pikitch, E.K., Punt, A.E., and Hilborn, R. 1994. A Bayesian approach to stock assessment and harvest decisions using the sampling/importance resampling algorithm. *Can. J. Fish. Aquat. Sci.* **51**: 2673–2688.
- Millar, R.B., and Meyer, R. 2000. Nonlinear state space modelling of fisheries biomass dynamics by using Metropolis-Hastings within Gibbs sampling. *Appl. Stat.* In press.
- Myers, R.A. 1997. Comment and reanalysis: paradigms for recruitment studies. *Can. J. Fish. Aquat. Sci.* **54**: 978–981.
- Myers, R.A., and Barrowman, N.J. 1996. Is fish recruitment related to spawner abundance? *Fish. Bull. U.S.* **94**: 707–724.
- Myers, R.A., and Mertz, G. 1998. The limits of exploitation: a precautionary approach. *Ecol. Appl.* **8**(Suppl. 1): s165–s169.
- Myers, R.A., Rosenberg, A.A., Mace, P.M., Barrowman, N.J., and Restrepo, V.R. 1994. In search of thresholds for recruitment overfishing. *ICES J. Mar. Sci.* **51**: 191–205.
- Myers, R.A., Bridson, J., and Barrowman, N.J. 1995. Summary of worldwide stock and recruitment data. *Can. Tech. Rep. Fish. Aquat. Sci.* No. 2024.
- Myers, R.A., Mertz, G., and Barrowman, N.J. 1996. Invariants of spawner-recruitment relationships for marine, anadromous, and freshwater species. *ICES C.M.* 1996/D:11.
- Myers, R.A., Hutchings, J.A., and Barrowman, N.J. 1997a. Why do fish stocks collapse? The example of cod in eastern Canada. *Ecol. Appl.* **7**: 91–106.
- Myers, R.A., Mertz, G., and Fowlow, S. 1997b. Maximum population growth rates and recovery times of Atlantic cod, *Gadus morhua*. *Fish. Bull. U.S.* **95**: 762–772.
- Pimm, S.L. 1991. The balance of nature. University of Chicago Press, Chicago, Ill.
- Punt, A., and Hilborn, R. 1997. Fisheries stock assessment and decision analysis: the Bayesian approach. *Rev. Fish Biol. Fish.* **7**: 35–65.
- Robinson, G.K. 1991. That BLUP is a good thing: the estimation of random effects. *Stat. Sci.* **6**: 15–51. With comments and a rejoinder by the author.
- Searle, S.R., Casella, G., and McCulloch, C.E. 1992. Variance components. John Wiley & Sons, New York.
- Suzuki, N., and Kitahara, T. 1996. Relation of recruitment to the number of caught juveniles in the ayu population of Lake Biwa. *Fish. Sci.* **62**: 15–20.
- Verbeke, G., and Lesaffre, E. 1996. A linear mixed-effects model with heterogeneity in the random-effects population. *J. Am. Stat. Assoc.* **91**: 217–221.

Appendix 1. Estimation in SAS

This appendix demonstrates how to fit the proposed model to data for a single species. In the SAS data step, a data set is created with three variables per observation: the name of the stock (i.e., population), *stock*, the number or biomass of spawners, *s*, and the survival, *surv*, respectively. The survival is $\log(R/S)$, where recruitment, *R*, has been multiplied by $SPR_F = 0(1 - p_s)$, so we will obtain estimates of $\bar{\alpha}$ in the appropriate units.

The SAS code for fitting the model with autocorrelated recruitment is

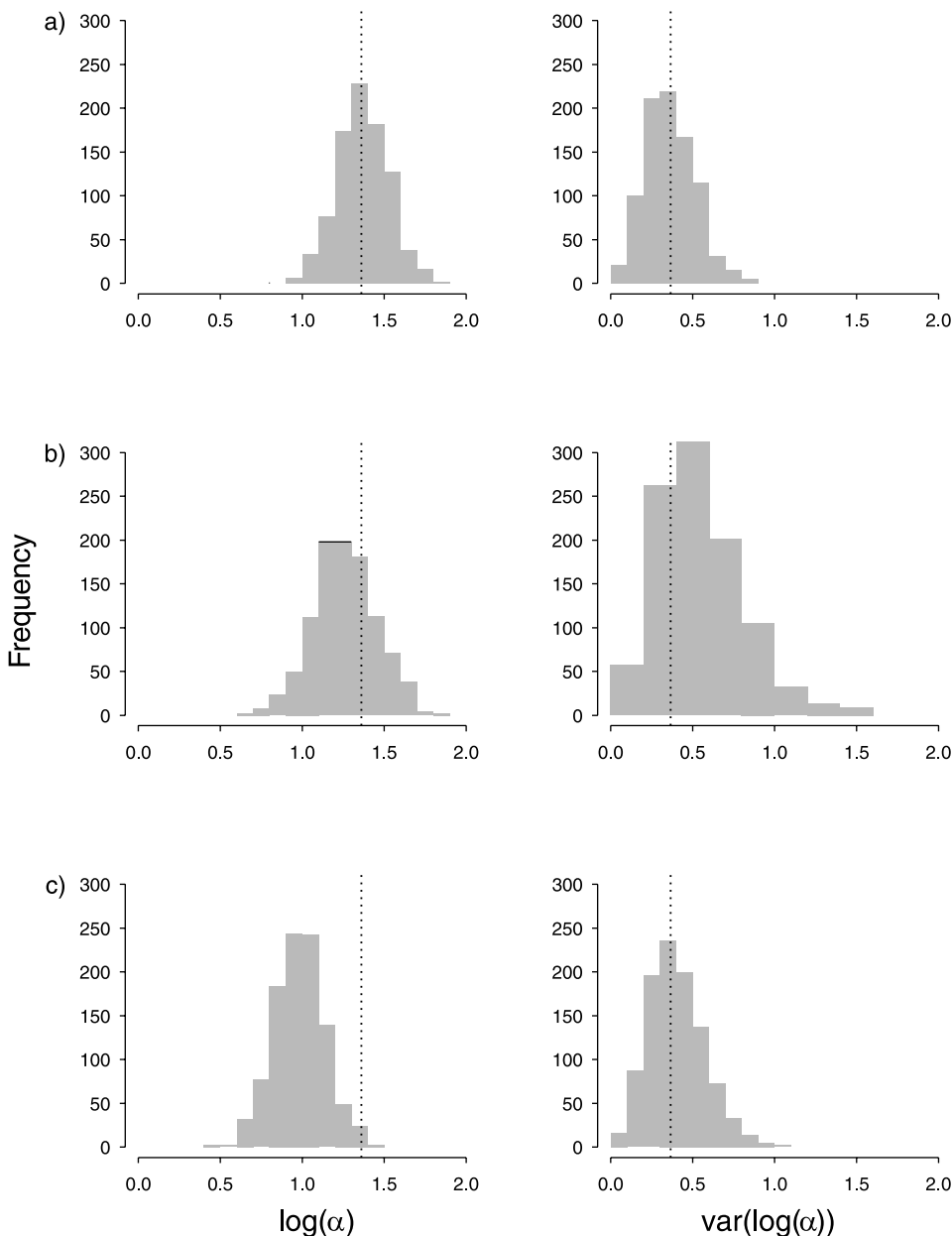
```
proc mixed method=reml;
  class stock;
  model surv= s*stock/solution;
  random int /subject=stock;
  repeated /subject=stock group=stock type=AR(1);
```

This model assumes autocorrelated errors and fits a separate first-order autocorrelation parameter and error variance for each stock. The method of estimation is REML.

Appendix 2. Robustness simulations

In order to test the robustness of the estimates from our model, we used simulations based on real data. The approach was to mimic the data for the 20 cod populations in the North Atlantic as closely as possible. In all cases, we used the observed spawner abundances, the estimated density-dependent parameters ($\hat{\beta}_i$), the estimated residual variance for each population, and the estimated mean (1.37) and variance (0.37) of the log α parameters. For each simulation, we randomly generated values for log α . Then, using the observed spawner abundances, the β_i s and the residual error variance that we produced simulated recruitment values that would closely match the actual data. We generated 1000 “realizations” of the 20 populations, randomly generating new log α values and then simulating recruitment in each case.

Fig. A1. Histograms of estimates of log α and σ_a^2 from simulations described in Appendix 2. The vertical dotted lines indicate the true estimates obtained using the data on 20 cod populations. Results from three different simulations are shown: (a) data simulated to match the model exactly, i.e., residuals and slope at the origin simulated from a lognormal distribution and expected recruitment given by a Ricker model, (b) residuals and slope at the origin simulated from a gamma distribution and expected recruitment given by a Ricker model, and (c) residuals and slope at the origin simulated from a lognormal distribution and expected recruitment given by a Beverton–Holt model.



We conducted three simulations. In each case, the model that we fit was a Ricker with lognormal distributions for both the error and the slope at the origin. In the first simulation, we generated data that matched this model exactly, i.e., a parametric bootstrap. In the second simulation, we generated data that was from a Ricker but had gamma (instead of lognormal) distributed residuals and slope at the origin. This was done to test the robustness of our inferences to misspecification of the probability distributions. In the last simulation, we generated data from a Beverton–Holt model with lognormal errors and slope at the origin. This was done to test the robustness of our inferences to misspecification of the spawner–recruitment model. From the histograms of the estimated $\log \tilde{\alpha}$ values, we can see that when our model was matched exactly by the data, the estimates were unbiased (Fig. A1a). When the distributional assumptions were violated, the value for $\log \tilde{\alpha}$ was underestimated, while the variance was overestimated (Fig. A1b). When the form of the model was incorrect, $\log \tilde{\alpha}$ was underestimated and the variance was relatively unbiased (Fig. A1c).